Sedimentation Effects on Triangular Short-Crested Flow-Measurement Weirs

Fred L. Ogden, M.ASCE[1]; Jesse N. Creel[2]; Edward W. Kempema[3]; and Trey D. Crouch[4]

Abstract: Flow-measurement weirs in natural channels experience sedimentation. Removing accumulated sediment is often impractical, prohibitively expensive, or both. This paper describes the results of hundreds of laboratory experiments conducted over a 6-year period to quantify the effect of sedimentation on the discharge coefficients for short-crested 120° and 140° triangular weirs over a range of flows, channel slopes, and different measurement positions along and across the channel. Two weir crest geometries were tested. These included the U.S. Department of Agriculture, Agricultural Research Service (ARS) design, and a modified ARS-type weir crest intended to reduce the frequency of plugging by floating debris called the Panama crest design. Two different weir crest thicknesses were tested in a hydraulics laboratory in two different flumes, with and without horizontal planar sedimentation, to identify the effects of sedimentation on discharge coefficients. Sediment transport was not considered. Results showed that in all cases sedimentation reduced the discharge coefficient by up to 10%. Channel slope had a relatively minor effect provided that the channel slope was less than or equal to 2% with a horizontal planar bed above the weir. Depth measurement position was of minor importance provided that the measurement was made out of the region of drawdown near the weir. The findings reported in this paper extend the usefulness of short-crested triangular weirs to conditions where the upstream pool is filled with sediment to the weir invert. **DOI: 10.1061/(ASCE)HE.1943-5584.0001528.**

Introduction

Weirs are generally of two types. The first type are constructed midchannel, oriented perpendicular to the flow, and are called measuring weirs (USBR 2001). The second type are oriented parallel to the flow on the sides of channels and only allow water to flow out when the water in the main channel reaches a certain height. Weirs of this second type are called side-channel weirs and are commonly used in storm drains and sewers. This study focused on measuring weirs.

Weirs are classified by their profile normal to the flow and crest geometry. Common weir profiles include rectangular, triangular, trapezoidal, logarithmic, and parabolic in the case of vertical roadway curves. There are three types of weir crests: sharp-edged, broad-crested, and short-crested. Sharp-edged weirs are generally made of a thin metal plate with a machined knifelike edge at the point in contact with the flow. Sharp-edged weirs are difficult to maintain in riverine settings because they are susceptible to damage by impacts by debris or ice. Broad-crested weirs are much thicker than sharp-edged weirs, often made of concrete, with weir crests long enough in the flow direction for the flow streamlines to become straight and parallel over the crest. Short-crested weirs are also frequently made of concrete and represent an intermediate crest length that is short enough in the flow direction that streamlines do not become parallel to the structure. In this paper, the term *short-crested* is used as per this definition. However, the terms *broad-crested* and *short-crested* have been used interchangeably (USBR 2001).

Agricultural Research Service-Type Triangular Weirs

This study was focused on triangular weirs of the Agricultural Research Service (ARS) variety with isosceles trapezoidal–shaped crowns, albeit with variable crest geometry. Triangular weirs are also called V-notch weirs. Fig. 1 shows the short-crested ARS-type weir geometric variables and crest dimensions. The ARS recommendation for short-crested weir thickness is 0.41 m (16 in.) (Brakensiek et al. 1979). Unlike the knifelike crest of sharp-edged weirs, the crowns of broad-crested and short-crested weirs can have different shapes owing to their thickness. Triangular weirs can be further classified by the angle of the V, which is shown as θ in Fig. 1. Triangular weir angles between 60° and 140° are most common. This study focused on 120° and 140° triangular short-crested weirs with isosceles trapezoidal crowns as shown in Section A-A in Fig. 1, because weirs of this geometry are commonly used in field settings.

With reference to Fig. 1, the theoretical equation for calculating the discharge, Q, over a triangular weir is

$$Q = C_d \frac{8}{15}\sqrt{2g}\tan\left(\frac{\theta}{2}\right)\left(h + \alpha\frac{V^2}{2g}\right)^{5/2} \tag{1}$$

Eq. (1) can be solved for the discharge coefficient as

$$C_d = \frac{\bar{Q}}{\frac{8}{15}\sqrt{2g}\tan(\frac{\theta}{2})\bar{H}_{\text{total}}^{5/2}} \tag{2}$$

where $H_{\text{total}} = h + \alpha V^2/2g$ is the total head assuming that the invert of the weir is at elevation $z = 0$. The overbar symbol above

[1]Cline Distinguished Chair of Engineering, Environment, and Natural Resources, Dept. of Civil and Architectural Engineering, Univ. of Wyoming, Laramie, WY 82071 (corresponding author). E-mail: fogden@uwyo.edu

[2]Consulting Engineer, Englewood, CO 80110; formerly, Graduate Student, Univ. of Wyoming, Laramie, WY 82071.

[3]Research Scientist, Dept. of Civil and Architectural Engineering, Univ. of Wyoming, Laramie, WY 82071.

[4]Ph.D. Candidate, Dept. of Environmental Engineering Sciences, Univ. of Florida, Gainesville, FL 32611; formerly, Graduate Student, Univ. of Wyoming, Laramie, WY 82071.

Note. This manuscript was submitted on May 25, 2016; approved on January 25, 2017; published online on May 2, 2017. Discussion period open until October 2, 2017; separate discussions must be submitted for individual papers. This paper is part of the ***Journal of Hydrologic Engineering***, © ASCE, ISSN 1084-0699.

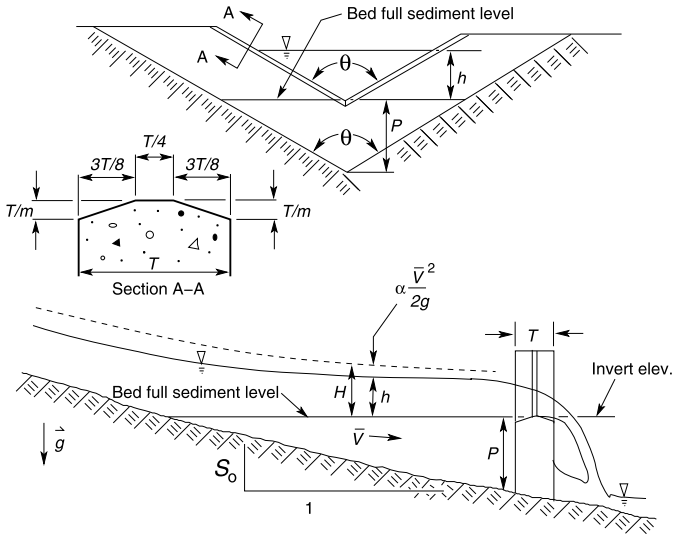

Fig. 1. Short-crested ARS-style triangular weir geometry definition sketch

the variables Q and H_{total} indicate that those variables are the result of repeat measurements, allowing minimization of the effects of measurement errors of Q and H_{total} on the dependent variable, C_d. Weirs in natural channels create local hydraulic control and provide the means to measure discharge through a water surface elevation measurement. The elevation of the weir invert, or low point of the V, is subtracted from the water surface elevation providing a static head measurement h as shown in Fig. 1.

Effects of Sedimentation

Weirs around the world are filling with or are full of sediment. The weir shown in Fig. 2 was constructed in Panama in 1979, is full of sediment, and is currently being used in a study of land-use effects on tropical hydrology (Ogden et al. 2013). Note the near planar sediment accumulation to the height of the weir invert. This weir is inaccessible by equipment because it is more than 2 km from the nearest road in a tropical forest. The objective of this study was to identify discharge coefficients that account for horizontal planar accumulations of sediment behind short-crested triangular weirs.

Fig. 2. Fully sedimented forest catchment weir in Soberania National Park, Panama, provided the impetus for this study (weir location: 9° 12′ 32″ N, 79° 46′ 46″ W) (image by Fred L. Ogden)

With reference to Fig. 1, the velocity head upstream from a triangular weir may be neglected when P, the vertical distance from the weir invert down to the bed of the channel on the upstream side of the weir, is at least 60% of the design static head $h_{\max}$. However, in natural channels that convey sediment, this condition is difficult to maintain. This is because the local control created by the presence of the weir causes flow deceleration with a corresponding decrease in sediment transport capacity. This results in sediment deposition in the pool upstream from the weir, decreasing P (Fig. 1) until $P = 0$. Depending on the sediment size and transport rate, weirs can fill with sediment during a single event. Further depending on site access and local conditions, routine removal of this accumulated sediment may be prohibitively expensive or impossible.

Literature Review

Numerous sources discourage using triangular weirs when the approach pool is filled with sediment up to the weir invert elevation. There are inconsistent recommendations regarding acceptable sediment accumulations. Guidance from the U.S. Bureau of Reclamation (2001) is that approach flow channels should be free of deposited sediment. Bos (1989) recommends that the minimum distance from the triangular weir invert to the channel bed, P in Fig. 1, should be at least 46 cm. The USDA Natural Resources Conservation Service (NRCS) (Brakensiek et al. 1979) recommends the channel upstream from short-crested triangular weirs be nearly straight and level for a distance of 13 m, and that $P \geq 0.15$ m. These conditions are unlikely to persist in natural channels with sediment transport. Both the USDA NRCS (Brakensiek et al. 1979) and the U.S. Bureau of Recommendation (2001) claim that deposition of material immediately upstream from the weir will cause flow measurement inaccuracies that are greatest at low measuring heads. Yet another guidance document from the World Meteorological Organization requires $P \geq 0.45$ m and h/P not to exceed 0.4 (WMO 1971).

Compared with rectangular weirs, triangular weirs require more head for the same discharge. This means that triangular weirs more accurately measure low flows than rectangular weirs (Brakensiek et al. 1979) and are therefore more suitable for use in research watersheds. Short-crested triangular weirs constructed of concrete were pioneered by the USDA in the 1930s and 1940s (Huff 1938, 1941a, b, 1942; Harrold and Krimgold 1943; Ree and Gwinn 1959; Holtan et al. 1962; Gwinn et al. 1968). In streams where sediment transport is significant, other types of devices such as supercritical flumes and drop-box weirs are recommended (Brakensiek et al. 1979). However, short-crested triangular weirs are considerably less expensive to construct.

The USDA ARS (Brakensiek et al. 1979) gives an empirical equation involving two empirical constants C_0 and C_1 to calculate C_d values for the ARS ($m = 8$, Fig. 1) weir crest for nonsedimented conditions insofar as those conditions can be identified

$$C_d = C_0 + C_1 \log\left(\frac{H}{T}\right) \tag{3}$$

Eq. (3) is applied piecewise over different ranges of HT^{-1}. The discharge coefficients reported in Brakensiek et al. (1979) include the constant $8/15\sqrt{2}$, which is equal to 0.7542, because those constants that appear in the derivation of Eq. (1) are missing from the weir equation published in Brakensiek et al. (1979). Dividing that constant out to adapt for this difference, Table 1 gives values of the

Table 1. Constants Used in Eq. (3) to Calculate Discharge Coefficients Consistent with Eq. (1) (Adapted from Brakensiek et al. 1979)

tan ($\theta/2$)	θ (degrees)	Range HT^{-1}	C_0	C_1
2	127	0.750–1.627	0.6361	0.0901
		1.628–3.716	0.6504	0.0224
		3.717–4.500	0.6817	−0.0325
3	143	0.750–2.379	0.6276	0.0938
		2.380–3.755	0.6530	0.0265
		3.756–4.500	0.6784	−0.0178
5	157	0.750–1.458	0.6319	0.1049
		1.459–3.769	0.6469	0.0135
		3.770–4.500	0.7516	−0.1683

constants C_0 and C_1 and their piecewise ranges of applicability in a form consistent with Eq. (1).

Discharge coefficients calculated using the constants in Table 1 are for nonsedimented conditions. The effect of sedimentation on ARS type ($m = 8$) weirs was studied by Mefford (1979) using a 1:5-scale model. However, Mefford's study was different than the present study in some key ways. Mefford's study was performed in a large recirculating flume with live sediment transport that in some tests had a sand dune upstream from the weir. In other tests by Mefford (1979), the sedimented bed was sloped, which led to supercritical flow approaching the weir crest and a rooster tail forming as flow passed over the weir, similar to the observations of Huff (1942) who attempted tests in steep channels using a 1:5-scale model. Mefford's study results were partially summarized by Saxton and Ruff (1976). As will be discussed in the results section, scale effects were observed in the 3:16-scale model of the ARS weir crest. It is likely that a model at 1:5-scale will be similarly affected.

Objectives

Hudson (2004) discussed the problem of sediment deposition that affects discharge measurements using weirs and offers the following solutions: (1) clear sediment after each flood event; (2) prevent sediment from reaching the structure; (3) derive a new calibration to reflect the deposition; or (4) redesign or replace the structure to allow sediment to pass. In many cases Solutions 1 and 4 are not reasonable because of difficulty accessing weir locations and expense. Sediment traps can be effective but they also require expensive dredging. Because in some cases dredging of accumulated sediment behind triangular weirs is impossible, a solution is needed. This study focused on Solution 3.

Laboratory and Apparatus

This study was performed in the Water Resources Laboratory at the University of Wyoming in two different size flumes. A small flume was used to test weirs with $T = 7.62$ cm (T = thickness of weir crest in the flow direction, Fig. 1), while the large flume was used to test weirs with $T = 20.3$ cm. These two flumes are described in the following sections.

Small Flume

The small flume shown in Fig. 3 is a tilting flume and was designed for this study to fit into limited space so it has a test section that is 3.4 m long and 1.47 m wide. This flume had a false floor that formed a V-shaped channel cross section. When a 120° weir was tested, a 120° false channel bed angle was installed with $PT^{-1} = 8.5/3$ during tests without sedimentation. Similarly, a 140° V-shaped channel was installed when the 140° triangular weir was tested with the same PT^{-1} value without sedimentation. This condition is equivalent to the recommendation by the U.S. Bureau of Reclamation (2001) that the triangular weir angle be selected that most closely matches the shape of the channel.

The small flume had a recirculating water supply system that included a 50-m^3-capacity sump with four 7.35-kW pumps configured to operate in parallel. These pumps fed a 25.4 cm nominal diameter supply line, which included a flow straightener, 15.88-cm-diameter orifice plate, and butterfly valve for flow-rate control. Four pressure taps around the circumference of the supply pipe

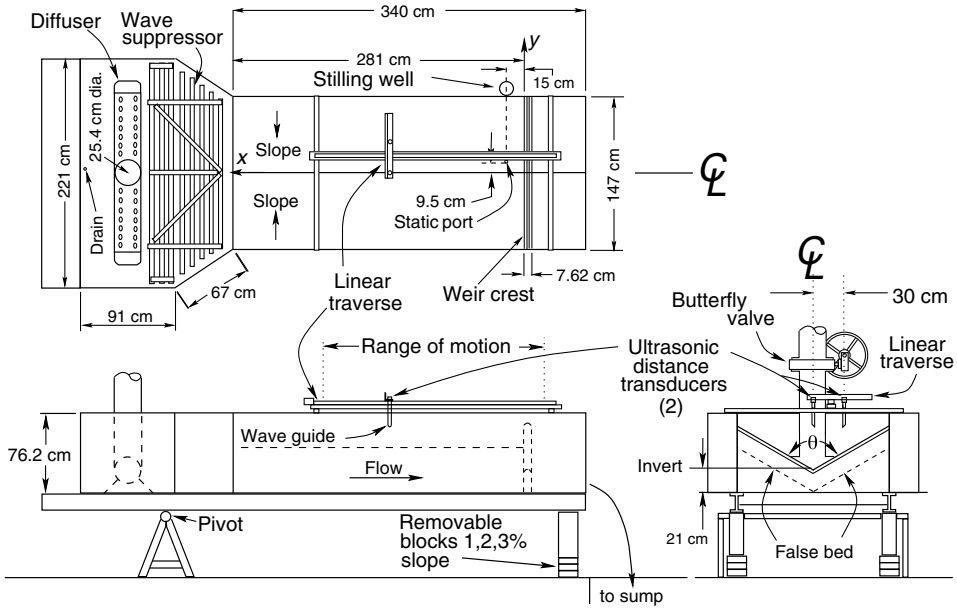

Fig. 3. Small flume used in tests with $T = 7.62$ cm; note coordinate system with origin at weir invert, x-direction upstream, y-direction lateral from centerline

upstream and downstream of the orifice plate were connected to a 2.3-m-tall differential water manometer. This orifice plate–manometer system was used to set flow rates at target values, and to validate operation of the weigh tank system. After overflowing the weir, the water flowing in this flume spilled into a return trough in the laboratory floor where it traveled to the splitter box above a weigh tank system.

The splitter box contained two 25.4-cm-diameter computer-controlled pneumatically actuated butterfly valves. Below each valve was a Fairbanks-Morse (Fairbanks Scales, Kansas City, Missouri) 10,880-kg-capacity scale tank instrumented with a load cell. Each scale tank was equipped with a floating grid cedar wave dampener, and a computer-controlled pneumatically operated 25.4-cm-diameter butterfly valve to drain the tanks to the sump, which was located below the weigh tanks. The weigh tank flow measurement program was written in *LabVIEW*, and featured adjustable fill, settling, and drain times.

The weigh tanks were calibrated twice during this study using a smaller 350-kg-capacity electronic scale that was calibrated using NIST-traceable standard weights by the Fairbanks-Morse company. On this smaller scale sat a tank with a volume of 0.33 m^3. Calibration of the large-scale tanks involved adding approximately 300 kg of water in steps up to their maximum capacity. The R^2 value between load cell output and weight of water in both large weigh tanks was 0.999.

Weir crests were constructed of planed cedar and coated with a thin uniform layer of room temperature vulcanization (RTV) silicone to help minimize surface tension effects and prevent absorption of water. A hook gauge was affixed to the flume for manual measurements of water surface elevation and for establishing the no-flow initial water surface condition as described in the methods section. Each test sequence of 17 discharges in the small flume took a full day for one person, and included six to eight repeat measurements of the discharge using the weigh tank system to minimize the effects of measurement errors.

Large Flume

The large flume shown in Fig. 4 was a recirculating flume 3.6 m wide with 13.6-m useable length between a wooden slat diffuser at the inlet and the pump intake at the downstream end. Flowing water was supplied by a 36.8-kW recirculating pump with motor speed control by a variable frequency drive. A 15.88-cm-diameter orifice plate installed in the 25.4-cm PVC pipe was connected to a 2.3-m-tall differential water manometer to provide flow measurement capability. The distance between the pump and orifice plate was more than 40 pipe diameters. The orifice plate was calibrated using the laboratory weigh tank system, and is identical to the orifice plate used in the small flume. A butterfly valve immediately upstream from the outlet diffuser allowed low-flow control and creation of back pressure to prevent cavitation near the orifice plate. When the head drop across the orifice plate exceeded the 2.3-m maximum provided by the differential water manometer, a U-tube differential mercury manometer with mercury traps was used that could measure 90-cm mercury head differential.

The large flume was constructed of wood framing and the walls would slightly deform as the water level varied. This caused the carriage that spanned the walls to move slightly. For this reason, the ultrasonic water level sensor was not mounted on the flume. Rather, it was mounted on an independently supported aluminum truss that spanned the flume. This provided water surface elevation readings that were immune from deformation of the flume walls.

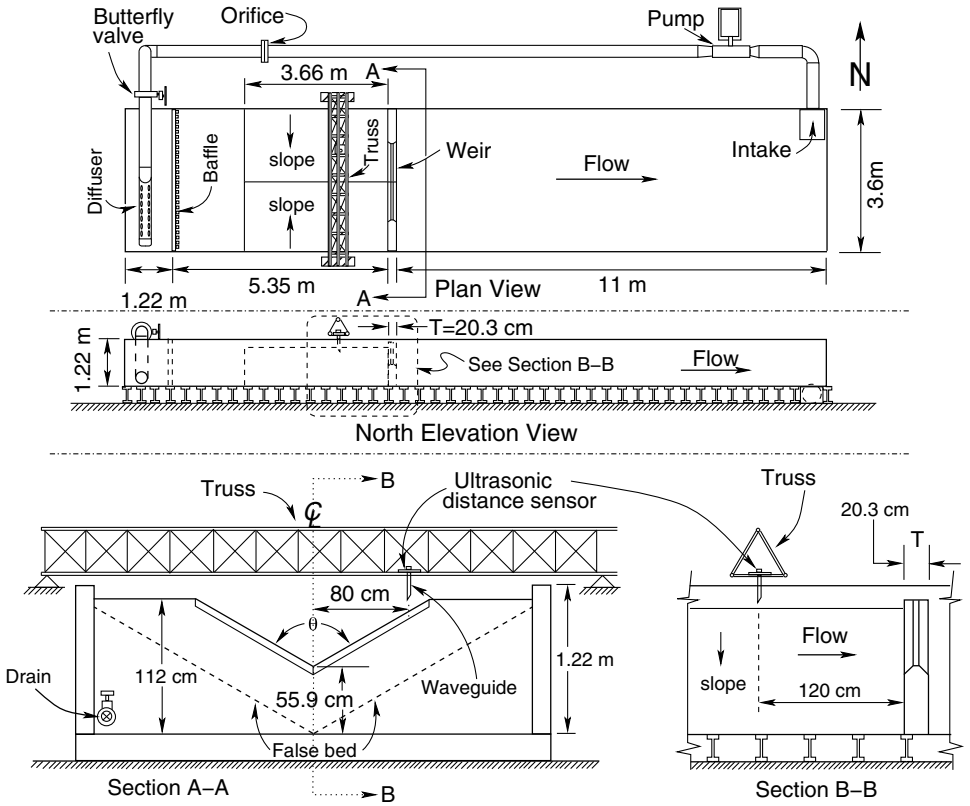

Fig. 4. Large recirculating test flume used in tests with $T = 20.3$ cm

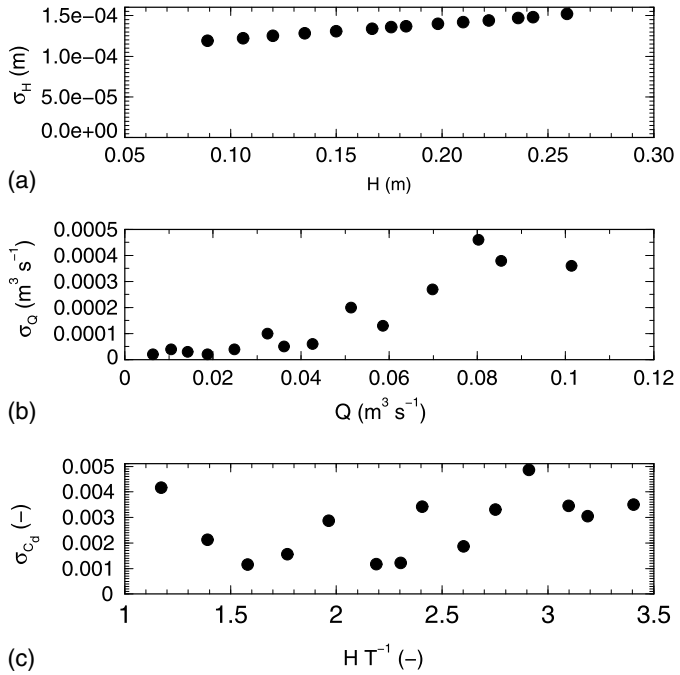

Fig. 5. Effect of measurement uncertainties in (a) water level (σ_H) and (b) discharge (σ_Q) on (c) the standard deviation of the discharge coefficient (σ_{Cd}); results shown in (c) were calculated using the data in (a) and (b) and Eq. (2) evaluated using Eq. (4), assuming that the covariance between Q and H measurements is zero

Instrumentation and Measurements

Using data from the small-flume system, the accuracy of manual differential manometer readings was established by analyzing the agreement between measured and actual manometer differential head from 629 readings between 10 and 220 cm. Weigh tank–determined flow rates allowed calculation of the actual manometer differential head. This analysis showed that the mean error in reading the water differential manometer was −0.04% and the mean absolute error was 1.2%. Flows that were too small to measure with the orifice plate and differential manometer were measured by taking repeated timed samples using a 19-L (5-gal.) bucket and weighing them. The time that the bucket was exposed to the flow was timed using a stopwatch with 0.1-s precision. According to a study comparing manual timing with electronic timing of 18.2-m (20-yd) sprints by 21-year-old males, manual timing on average led to −0.20 s difference with a standard deviation of 0.049 s (Ebben et al. 2009). Timing a bucket filling versus timing of a sprinter are similar in that the person doing the manual timing must estimate both a start and a running stop time. Assuming −0.20 s time measurement error with a stopwatch, this corresponds to −1.1% error in flow rate at 1 L s^{-1}, and −12.5% at 10 L s^{-1} when using a 19-L bucket. Six repeated measurements were made, and these repeat measurements reduced the flow uncertainty at 10 L s^{-1} to 5.1%.

Ultrasonic distance sensors were used to measure water levels. These were U-Gage (Banner Engineering, Minneapolis, Minnesota) model number T30UX1AQ8 sensors, fitted as per manufacturer recommendation with wave guides fabricated from 24-cm lengths of 19-mm-diameter PVC pipe with ends cut at a 45° angle to avoid standing waves. These wave guides served to decrease the dispersion of the ultrasonic signal and hence the diameter of the detection circle on the water surface. A *LabVIEW* program read the sensors at approximately 7 Hz. A total of 100 repeat distance measurements were performed to allow statistical analysis. These sensors were used in both flumes. In the small flume, two sensors were installed on a computer-controlled traverse driven by an MDrive (Schneider-Electric Motion USA, Marlborough, Connecticut) model MD14MRQ23C7 stepper motor. With reference to Fig. 3, one sensor was installed over the centerline of the flume, and the second was installed 30 cm (4T) off-center. A *LabVIEW* computer program provided stepper motor control.

Fig. 5(a) shows the standard deviation of distance measurements as a function of water level based on analysis of approximately 600 sets of 100-point samples per set. Increasing depth decreases the distance from the water surface to the sensor, and the standard deviation increases. This was likely due to increased turbulence that caused capillary waves on the free surface because larger depth corresponds with higher discharge.

Flow measurements in the small flume used the weigh tank system. Dynamic testing of the weigh tank system involved repeated measurements of flow and comparison of the results provided by each weigh tank. Results of 19 to 24 pairs of flow comparisons between the two weigh tanks at 13 different constant flow rates are listed in Table 2. Fig. 5(b) plots the standard deviation of the weigh tank comparisons divided by $\sqrt{n}$ with $n = 6$, which was the minimum number of weigh tank flow measurements used during the tests.

The results shown in Fig. 5(b) show an increase in standard deviation with increasing flow rate. The errors in both the flow-rate and water level measurements are normally distributed and

Table 2. Results of Weigh Tank Intercomparison Test

Nominal Q (m^3 s^{-1})	Number of data pairs	Mean south weigh tank Q (m^3 s^{-1})	Mean north weigh tank Q (m^3 s^{-1})	Mean absolute difference (m^3 s^{-1})	Standard deviation (m^3 s^{-1})
0.0040	23	0.0040	0.0040	0.00006	0.00002
0.0064	23	0.0064	0.0063	0.00010	0.00004
0.0105	19	0.0106	0.0104	0.00015	0.00003
0.0143	24	0.0144	0.0142	0.00018	0.00002
0.0188	21	0.0189	0.0187	0.00019	0.00004
0.0249	22	0.0250	0.0248	0.00018	0.00010
0.0324	22	0.0325	0.0323	0.00019	0.00005
0.0361	22	0.0361	0.0361	0.00010	0.00006
0.0426	20	0.0425	0.0426	0.00028	0.00020
0.0513	20	0.0513	0.0513	0.00019	0.00013
0.0586	22	0.0585	0.0588	0.00042	0.00027
0.0698	23	0.0695	0.0701	0.00063	0.00046
0.0802	23	0.0801	0.0804	0.00056	0.00038
0.0854	22	0.0854	0.0854	0.00049	0.00036
0.1014	23	0.1013	0.1016	0.00064	0.00049

uncorrelated, so the transmission of error method was used to approximate the total measurement system variance (Montgomery et al. 2007) using Eq. (4)

$$\sigma^2(C_d) = \left[\frac{\partial C_d}{\partial Q}\right]^2 \sigma^2(Q) + \left[\frac{\partial C_d}{\partial H_{\text{total}}}\right]^2 \sigma^2(H_{\text{total}}) \qquad (4)$$

In the case of triangular weirs, Eq. (1) was manipulated to produce the partial derivative terms for use in Eq. (4). The use of Eq. (4) assumes that there is no covariance between the ultrasonic water level sensors and the weigh tank system. Fig. 5(c) shows the result of the measurement system errors on the calculated discharge coefficients.

The results shown in Fig. 5(c) indicate that system measurement errors are a relatively minor component of the uncertainty in the C_d values. Other potential measurement error sources include the initial nonflowing water surface elevation when the water surface is equal with the weir invert and the kinetic energy correction factor, α.

Methods

With reference to Fig. 1, variables manipulated in this study include channel slope ($S_o = 0$, 1, 2, 3%), sedimentation condition ($P = 0.6H_{\max}$, $P = 0$), crest shape (ARS: $m = 8$, Panama: $m = 4$), weir angle ($\theta = 120°$, 140°), depth measurement location along the channel ($2 \le xT^{-1} \le 18$, where x is the along-stream distance from the weir face), and lateral location from weir centerline ($yT^{-1} = 0$, $yT^{-1} = 4$). To avoid scale effects at smaller values of normalized flow depth HT^{-1}, two weir thicknesses, T, were used in this study: 20.32 and 7.62 cm in two different flumes.

Using the crest thickness T as a fundamental length variable in Froude similarity theory for free-surface flows, these different crest thicknesses can be considered different scales. Field values of T for these short-crested weirs range from 20.32 to 43 cm. Therefore, the range of scales tested varied from 1:1 in the case of the Panama weir crest where $T = 20.32$ cm in the field, to 1:5.64 in the case of the ARS weir crest with field thickness 43 cm when tested in the laboratory with $T = 7.62$ cm. The use of a scale as near as possible to 1:1 helps to avoid scale effects due to dissimilarities in the Reynolds number and momentum flux and pressure forces in the model and prototype that can affect the character of flow at the weir crest for short-crested weirs.

Determination of No-Flow Water Surface Elevation

Accurately establishing the water level datum that represents the weir invert elevation as read by the ultrasonic distance transducer(s) is extremely important. Errors less than 1 mm cause large errors in discharge coefficient, particularly at lower values of HT^{-1}. These errors are plotted in Fig. 6 for the test conditions in the small flume. Fig. 6 shows that a 1-mm error in the initial no-flow water surface elevation causes from 2% to almost 6% error in calculated C_d depending on HT^{-1}.

Relying on visual identification of the no-flow water surface elevation upon drain down is not reliable because of surface tension effects in the weir invert. At the start of each day's testing, a surveying level was used to survey the invert elevation of the weir being tested using a mechanics rule graduated at 0.4 mm as a surveying rod. At close distance this mechanic's rule could be read to a precision of 0.2 mm. If this precision represents the standard error of this effect on the discharge coefficient, then its portion of the error budget is less than 0.5% over the range of HT^{-1} tested.

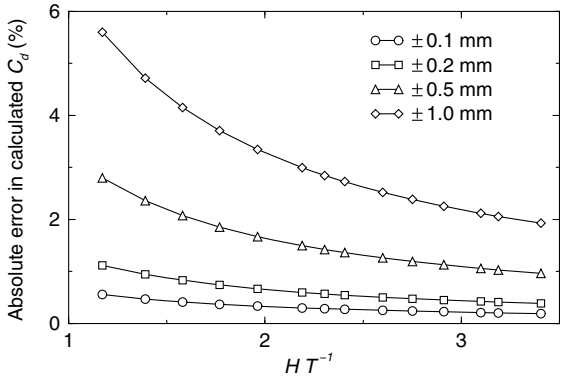

Fig. 6. Effect of initial $Q = 0$ water surface elevation measurement error on calculated discharge coefficient in percent, over a range of measured water surface elevations in the small flume with $T = 7.62$ cm

If present, pea gravel was scooped away from the areas where the ultrasonic sensors made measurements to a depth of 1 to 2 cm so that the pea gravel did not interfere with the ultrasonic sensor calibration. The hook gauge was set to the same elevation as the weir invert by again surveying using the mechanics rule within 0.2-mm precision as the survey rod. The flume was then filled with enough water to start flow over the weir. The water supply was shut off, and the flume drained using a drain valve until the hook gauge point became exposed. The drain valve was closed immediately to establish the no-flow water surface elevation that was used to calibrate the ultrasonic distance transducer zero elevation datum. In the case of the small flume, the data acquisition program was run, which collected data representing no-flow initial water surface elevations from the computer control traverse at all 22 measurement locations.

A similar protocol was established in tests with the large flume. The no-flow initial condition was established by surveying the weir invert elevation and using that observation to set a hook gauge. Water was added to establish flow over the weir and drained using a drain valve until exposure of the tip of the hook gage. The *LabVIEW* data acquisition program was run to collect 100 water surface elevation points over an approximately 14-s period with 7-Hz sampling frequency. The average of these points represented the no-flow zero water surface datum. These data were useful for detecting leaks in the large flume because filtered ultrasonic distance transducer measurements can reveal extremely small changes O(10 μm) in the water surface elevation. Continuous change in water surface elevation after closing the drain indicated a leak.

Standard Test Methodology

In general, tests involved increasing flows throughout the day. The differential manometer was used to establish the flow rate. In tests in the small flume, the weigh tank program was run continuously, producing a new flow-rate measurement approximately every 3 min. When the flow rate reached an equilibrium, the *LabVIEW* data acquisition program was run, sampling the centerline and 30-cm off-centerline ultrasonic distance sensors at 7 Hz, collecting 100 data points at each position. The computer then commanded the linear traverse to move 15 cm upstream, and repeat the 100 distance measurements. Eleven positions spaced 15 cm apart along the length of the flume were sampled, resulting in a total of 22 water level measurement locations. The output of a day's tests included ASCII files containing 100 water level measurements

(a) (b)

Fig. 7. Fully sedimented bed conditions after tests in (a) 120° $T = 7.62$ cm Panama weir crest in small flume; (b) 140° $T = 20.32$ cm ARS weir crest in large flume; slight scour observed in pea gravel near weir invert in both cases; note computer-controlled linear traverse in (a); ultrasonic distance sensors are identifiable by the PVC wave guides that are cut with 45° ends [scale units 0.031 m (0.1 ft)] [images by Fred L. Ogden; Edward W. Kempema appears in (b)]

at 22 locations for each of the 17 discharges tested, including the no-flow set.

Because flow measurements in the large flume depended upon either timed volumetric or orifice flow–differential manometer measurements, the ultrasonic water level sensor was used to determine steady state. The *LabVIEW* program continuously plotted water level in an on-screen graph versus time. After an increase in flow rate, the water level was observed until it remained unchanged for at least 2 min. At that time, a *LabVIEW* program was activated to read the one ultrasonic distance sensor at 7-Hz frequency to collect 100 data points. Those data points were written to a file. The differential manometer was read before and after the running of the distance logging program. These two readings were entered into the spreadsheet. If either the flow or the water surface elevation experienced a noticeable change, then the measurement was repeated. In later tests, a hook gauge reading was taken before and after running the *LabVIEW* program as an independent check of steady-state conditions.

Analysis of Water Surface Elevation Measurements

A computer program was written that performed several key data processing functions. First, acting on the 100 repeat measurements of water level, it performed outlier detection and normality testing using the Shapiro and Wilk (1965) test, discarding extreme outliers to ensure data normality with $p = 0.05$, then calculating the first four moments of the distribution. Occasionally some sequences of 0.0 distance measurement occurred in the output due to latency and buffer synchronization errors. In no case were fewer than 20 values used in computation of statistics, and most often fewer than 10 outliers were removed. Second, this program used the no-flow water level readings to calibrate the zero-head datum for each ultrasonic sensor position and each flow. This datum was subtracted from water level measurements during each flow to calculate the velocity and total head H_{total}. Finally, the program calculated the discharge coefficients, C_d, and wrote output files of C_d versus Q for each measurement position, for velocity-head corrected (H_{total}) and uncorrected (h) measurements.

Approach flow velocity profiles were not measured. Mefford (1979) performed multiple measurements of α in several different channel shapes above triangular short-crested weirs in a 2.44-m-wide flume. Chow (1959) recommended α values between 1.03 and 1.36, while Brakensiek et al. (1979) assumed $\alpha = 1.33$. Because of similarities with Mefford's experimental geometry and flows, Mefford's (1979) average measured value $\alpha = 1.115$ was applied in the present study.

Repeatability of experiments was challenging because of errors such as those related to initial water surface elevation measurements or other unpredictable factors. Repeat experiments allowed quantification of the uncertainty of the C_d values. The number of repeat experiments varied from four to nine depending on test condition. The 95% confidence intervals ($p = 0.05$) were computed using the Student's t distribution from the results of n independent C_d measurements with standard deviation s as

$$\bar{C}_d \pm t_{0.05,n-1}\left(\frac{s}{\sqrt{n}}\right) \tag{5}$$

Simulation of Sedimentation

Sedimentation was simulated using granular material near the weir face, but with a false bed elsewhere as shown in Figs. 7(a and b). In the case of the small flume, $T = 7.62$ cm, shown in Fig. 7(a), where the variable slope tests were performed, the shape of the false bed depended upon the slope to keep the surface of the sedimented bed horizontal. The pea gravel shown in Fig. 7(a) extended upstream 45 cm from the weir.

The large flume with weir crest thickness $T = 20.3$ cm is shown in Fig. 7(b), where medium sand was placed within approximately 61 cm of the weir face. The purpose of this sand was to allow the bed to deform because this weir crest thickness is very near the prototype scale, and sediment transport is likely, justifying a moveable bed. Despite the relatively high mobility of medium sand, at the end of the test a relatively small amount of sand was lost. In later tests in the large flume, pea gravel was used in the large flume instead of medium sand. Approximately the same amount of erosion was observed near the weir invert [Fig. 7(b)]. In the large flume the bed was horizontal for a distance of 2.4 m upstream from the weir, and the channel side slope was the same as the weir angle θ as shown in Fig. 1.

Results and Discussion

Because of the large number of test variables and the desire to place confidence bounds on the results using results from repeat experiments, more than 300 tests were performed. Crest geometry was identified as having a dominant effect on the performance of the

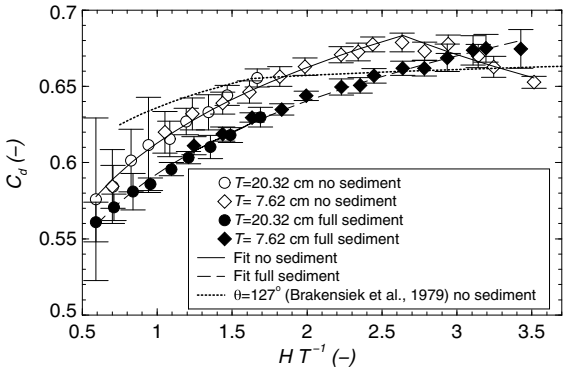

Fig. 8. Results of tests on $\theta = 120°$ USDA-ARS weir crest ($m = 8$) with and without sedimentation; the USDA-ARS curve for 127° weirs (Brakensiek et al. 1979) is shown for comparison

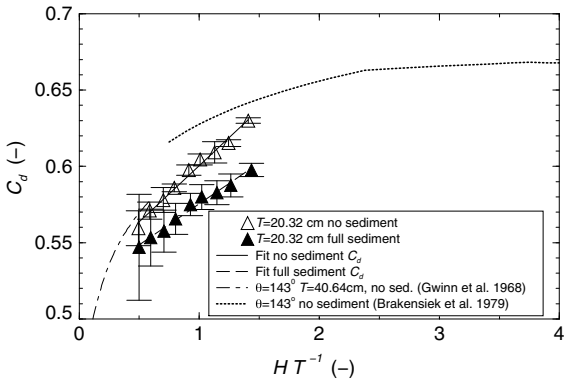

Fig. 9. Results on tests of $\theta = 140°$ USDA-ARS crest ($m = 8$) with and without sedimentation; the USDA-ARS curve for 143° weirs (Brakensiek et al. 1979) is shown for comparison, as are data from Gwinn et al. (1968) for $HT^{-1} \leq 0.6$

weirs. For this reason the results are presented separately for the two weir crest geometries tested. With reference to Fig. 1, the ARS crest has $m = 8$, while the Panama crest has $m = 4$.

ARS Weir Crest

Fig. 8 shows the results of tests on a 120° triangular angle ARS crest weir. The USDA-ARS discharge coefficient (Brakensiek et al. 1979) for a 1:2 ($\theta = 127°$) weir angle is plotted for comparison purposes. The USDA discharge coefficient curve is in approximate agreement. The rise in C_d value seen in the 3:16-scale model with $T = 7.62$ cm model between $1.9 < HT^{-1} < 2.64$ might be due to scale effects. This conclusion is based on the observation that the 140° 3:16-scale ARS crest results were scale affected, as discussed in the next several paragraphs. The agreement between these weir tests at 1:2 and 3:16 scale provides some confidence in the results for $HT^{-1} < 2$.

The modeled C_d curves shown in Fig. 8 are given by the set of Eqs. (6*a*) and (6*b*) for the no-sediment condition

$$C_d = 0.6128\left(\frac{H}{T}\right)^{0.1124} \qquad 0.58 \leq \left(\frac{H}{T}\right) < 2.64 \qquad (6a)$$

$$C_d = 0.7875\left(\frac{H}{T}\right)^{-0.146} \qquad 2.64 \leq \left(\frac{H}{T}\right) < 3.51 \qquad (6b)$$

In the case of the fully sedimented condition in Fig. 8, one empirical curve fits the data over the range from $0.59 \leq HT^{-1} \leq 3.43$. Eq. (7) describes that curve

$$C_d = 0.5927\left(\frac{H}{T}\right)^{0.1115} \qquad (7)$$

Fig. 9 shows measured C_d curves for the 140° ARS weir crest with and without sedimentation with a weir crest $T = 20.32$ cm, which resulted in a scale of 1:2. A series of tests were performed at 3:16 scale, but those results did not agree with the 1:2-scale results, leading the authors to conclude that at 3:16 scale there were significant scale effects that caused differences in the pressure distribution on the crest. This was likely due to differences in vertical momentum fluxes near the crest. Therefore, the 3:16-scale results are not shown in Fig. 9.

With $T = 20.32$ cm in the case of no sediment, simple linear regression fits the observations over the range of tested HT^{-1} values

$$C_d = 0.527 + 0.0739\frac{H}{T} \qquad 0.50 \leq \left(\frac{H}{T}\right) \leq 1.40 \qquad (8)$$

When the weir is fully sedimented the linear equation that fits the C_d measurements is

$$C_d = 0.522 + 0.0537\left(\frac{H}{T}\right) \qquad 0.49 \leq \left(\frac{H}{T}\right) \leq 1.44 \qquad (9)$$

Two other curves are plotted on Fig. 9. One is the recommended C_d curve by Brakensiek et al. (1979) for the nonsedimented 143° ARS weir. That curve nears the measured curve from the present study near the upper end of the range of HT^{-1} values tested. Also plotted on Fig. 9 are C_d values measured by Gwinn et al. (1968) for $HT^{-1} < 0.6$ with $T = 40.64$ cm (1:1 scale). Those values agree well with measurements from the present study, and support the notion that the 1:2-scale tests in the present study did not suffer from appreciable scale affects. For $HT^{-1} > 1.4$, and nonsedimented conditions, the Brakensiek et al. (1979) C_d curve should be used. In the case of sedimented conditions, the Brakensiek et al. (1979) C_d values should be reduced by 5.1%, which is the difference observed in the present study between nonsedimented and sedimented tests at 1:2 scale and $HT^{-1} = 1.4$, and is also exactly equal to the difference between the 3:16-scale tests with and without sedimentation over the range of $1.5 < HT^{-1} < 2.8$.

The 3:16-scale 140° ARS weir model results were not plotted in Fig. 9 because they were scale-affected. However, the effect of sedimentation on C_d values due to sedimentation effects measured at 3:16 scale agreed with the difference due to sedimentation in the half-scale model where the results overlap at $HT^{-1} = 1.4$.

Panama Weir Crest

The Panama weir crest, with its steeper crest facet slope, more closely approximates a rounded crest. The measured C_d values for the 120° Panama weir crest are shown in Fig. 10. The modeled empirical equations that fit the C_d values without sedimentation are

$$C_d = 0.665\left(\frac{H}{T}\right)^{0.1052} \qquad 0.25 \leq \left(\frac{H}{T}\right) \leq 0.959 \qquad (10a)$$

$$C_d = 0.663\left(\frac{H}{T}\right)^{0.0353} \qquad 0.959 \leq \left(\frac{H}{T}\right) \leq 2.88 \qquad (10b)$$

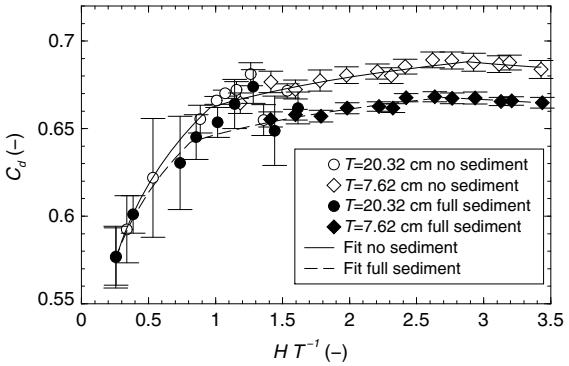

Fig. 10. Results of tests on $\theta = 120°$ Panama weir crest ($m = 4$) with and without sedimentation

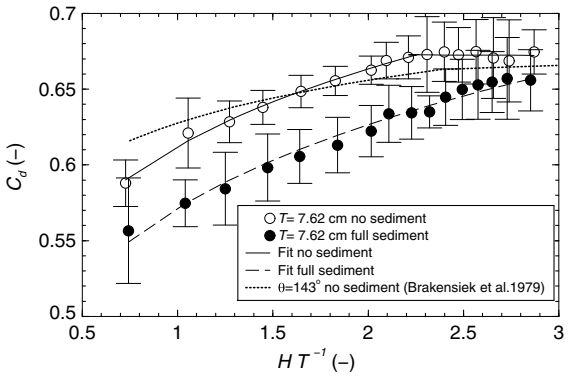

Fig. 11. Results of tests on $\theta = 140°$ Panama weir crest ($m = 4$) with and without sedimentation; the USDA-ARS curve for 143° weirs (Brakensiek et al. 1979) is shown for comparison

$$C_d = 0.707\left(\frac{H}{T}\right)^{-0.0255} \qquad 2.88 \le \left(\frac{H}{T}\right) \le 3.43 \qquad (10c)$$

When the 120° Panama weir is fully sedimented, the empirical fit equations that fit the C_d measurements are

$$C_d = 0.655\left(\frac{H}{T}\right)^{0.0935} \qquad 0.25 \le \left(\frac{H}{T}\right) \le 0.814 \qquad (11a)$$

$$C_d = 0.647\left(\frac{H}{T}\right)^{0.0325} \qquad 0.814 \le \left(\frac{H}{T}\right) \le 2.72 \qquad (11b)$$

$$C_d = 0.681\left(\frac{H}{T}\right)^{-0.0195} \qquad 2.72 \le \left(\frac{H}{T}\right) \le 3.43 \qquad (11c)$$

The C_d values shown in Fig. 10 exhibit a discontinuity near $HT^{-1} = 1.3$. This discontinuity is due to a change in flow regime and is discussed subsequently.

Fig. 11 shows the measured C_d values for the 140° Panama weir crest. In the nonsedimented case, the C_d values are empirically fit by two power-law relations for the range of HT^{-1} values tested

$$C_d = 0.612\left(\frac{H}{T}\right)^{0.1159} \qquad 0.72 \le \left(\frac{H}{T}\right) \le 2.253 \qquad (12a)$$

$$C_d = 0.674\left(\frac{H}{T}\right)^{-0.0017} \qquad 2.253 \le \left(\frac{H}{T}\right) \le 2.87 \qquad (12b)$$

The fully sedimented 140° Panama weir crest is fit by a single power-law equation over the range of HT^{-1} values tested

$$C_d = 0.571\left(\frac{H}{T}\right)^{0.1332} \qquad 0.74 \le \left(\frac{H}{T}\right) \le 2.85 \qquad (13)$$

Also plotted on Fig. 11 is the C_d relation suggested by Brakensiek et al. (1979) for the 143° ARS weir crest without sedimentation. Coincidentally, it agrees reasonably well with the 140° Panama weir crest C_d values measured without sedimentation.

Crest-Shape Effects

In both the sedimented and nonsedimented cases, the 120° Panama weir crest exhibited a sudden drop in discharge coefficient from 0.682 to 0.658 when HT^{-1} reached and exceeded approximately 1.3. A series of measurements and observations involving small increases in discharge identified the cause of this sudden decrease in C_d in the case of increasing discharge. Repeat photography of the nappe showed differences in the trajectory and the aeration of the nappe occurring with a very small change in discharge as shown in Fig. 12.

Figs. 12(a and b) show two significant observed changes that occurred between $Q = 0.0985$ m^3 s^{-1} and $Q = 0.1014$ m^3 s^{-1}. The first was that in Fig. 12(a), the nappe is in contact with the downstream facet of the weir crest. In Fig. 12(b), there is evidence of flow separation from the downsloping facet because air has invaded the space between that facet and the underside of the nappe. The second change observed is that the trajectory of the nappe is different. Comparing the trajectory of the nappe against the structural timbers behind the nappe in Fig. 12(a) clearly shows that the trajectory of the nappe is considerably steeper there than in Fig. 12(b).

The effect of the condition shown in Fig. 12(a) is to create a region of subatmospheric pressure on the downsloping facet of the weir crest. This allows the crest to have a slight siphon effect and acts to increase the discharge coefficient. The slight 0.0029 m^3 s^{-1} increase in flow corresponds to a sufficient increase in flow momentum to allow the flow to separate from the downsloping crest facet. The subsequent loss of suction results in a sudden decrease in C_d from 0.682 to 0.658, a decrease of 3.5%, as the data in Fig. 13 show.

The geometry of the Panama and ARS weir crests offer three opportunities for such transitions as shown on inset figures labeled 1–4 on Fig. 13. There is a similar, albeit not as abrupt, decrease in C_d seen in Fig. 8 for the 120° ARS weir for HT^{-1} slightly larger than 2.5. This strong tendency to separate from the downsloping facet of the weir crest creates a hysteresis in weir behavior, which is undesirable. As shown in Fig. 13, the hysteresis occurs in the region $1.1 < HT^{-1} < 1.4$. As the results in Fig. 10 show, it is not particularly pronounced compared with the remainder of the curve. When $HT^{-1} > 1.4$, this weir is well behaved with a near-constant C_d value for both sedimented and nonsedimented conditions.

It is likely that the flow will transition from Condition 1 directly to Condition 4 in the case of the ARS weir crest because of its flatter crest design and more acute first facet angle (Fig. 12). That said, this transition was not seen in the $T = 7.62$ cm tests of the ARS weir crest that are not reported because of scale effects, and the failure to see this transition might be another scale effect. Furthermore, this transition was not seen in the $T = 20.32$ cm tests, perhaps because of the limited flow rate in the apparatus.

Fig. 12. Evidence of cause of C_d hysteresis seen in the Panama weir crest ($m = 4$) 120° results; note difference in nappe trajectory and air entry below nappe on downstream facet of weir crest in (b): (a) $Q = 0.0985$ m^3 s^{-1} and $C_d = 0.682$; (b) $Q = 0.1014$ m^3 s^{-1} and $C_d = 0.658$; data from $T = 20.3$ cm tests without sedimentation (images by Fred L. Ogden)

Channel Slope Effects

The sedimented test condition imposed a horizontal bed upstream from the weir. Under this condition, the slope of the channel was found to have a negligible effect except in the case of $S_o = 3\%$ slope. The results for $S_o = 0$, 1, and 2% were virtually identical and were combined to increase the sample size and decrease the width of the 95% confidence bounds. The C_d values measured in $S_o = 3\%$ channels were within 2% of the values measured in less steep channels. A 3% channel slope is a very steep channel. Those results are presented in Creel (2013) for the Panama weir crest shape.

While Saxton and Ruff (1976) reported that channel bed slope S_o had an effect on their measured C_d values, they did not show data points on their curves of discharge versus head. Plus, the effect of channel bed slope reported by Saxton and Ruff (1976) is greater than the reported effect of sedimentation, the exact opposite of the findings in the present study. The authors can only say that the statistical analysis enabled by repeated experiments at each flow condition allowed quantification of the uncertainty in the results.

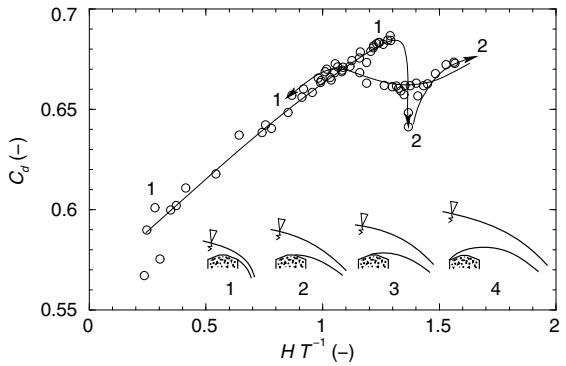

Fig. 13. Results of experiment designed to discover reason for abrupt change in discharge coefficient for 120° Panama weir crest ($m = 4$) and $T = 20.4$ cm; transitions to separate Conditions 3 and 4 occur at larger values of HT^{-1} than shown

Measurement Position Effects

Referring to the coordinate system shown in Fig. 3, water level measurements at 11 different positions upstream from the weir face in the small flume allowed testing of the effect of longitudinal position. Based on calculated discharge coefficients when the weir is free of sediment, a single discharge coefficient is valid for measurements in the range of $6 \le xT^{-1} \le 18$ upstream from the weir because the discharge coefficients varied by less than 2%. In the range of $2 \le xT^{-1} \le 4$, separate discharge coefficients are calculated because of the influence of drawdown near the weir. When the weir was full of sediment C_d was single valued from $8 \le xT^{-1} \le 18$ because the calculated values varied by less than 2%. However, between $2 \le xT^{-1} \le 6$, discharge coefficients calculated differed by more than 2%.

The second water level measurement position variable tested was lateral position. Measurements were made at two lateral locations. The first was along the channel centerline, and the second was along the line $yT^{-1} = 4$. The results are identical to those for longitudinal position. In the nonsedimented case, a single C_d value was found for both $yT^{-1} = 0$ and $yT^{-1} = 4$ when $6 \le xT^{-1} \le 18$. When the weir was full of sediment the range of single C_d values was $8 \le xT^{-1} \le 18$. Therefore, for the range of HT^{-1} tested in this study, measurements of water level at any location across the channel for $8 \le xT^{-1} \le 18$ is acceptable for both weir crests.

Conclusions and Future Research Recommendations

The effect of sedimentation in all cases studied was to reduce the discharge coefficient. The reduction was predictable and consistent, which indicated that the effect of sedimentation can be accounted for when using sedimented short-crested triangular weirs for flow

measurements. This conclusion holds for triangular weirs in channels with a trapezoidal cross section with slope less than or equal to 2%, with short crest of the ARS ($m = 8$) or Panama ($m = 4$) type, and with 120° or 140° weir angle θ. Those results are shown in Figs. 8–11. Empirical C_d functions are provided that fit the data over the tested range of HT^{-1} values.

The recommended C_d values for the USDA-ARS 143° triangular weir without sedimentation (Brakensiek et al. 1979) agree with the values measured in the present study with differences generally less than 5%. The present study included an exhaustive literature review that included communications with the USDA-ARS, and no single report was found describing the methodology and data used to produce the C_d values recommended in Brakensiek et al. (1979). Rather, it seems that the curves of recommended C_d values from Brakensiek et al. (1979) come from a variety of internal ARS reports.

The authors have high confidence in the $T = 20.32$ cm results, as evidenced by the thin 95% confidence intervals. The similarity between the nonsedimented curve reported in the present study and the results by Gwinn et al. (1968) for small values of HT^{-1}, and the similarity between the curve reported from the present study and the recommended curve by Brakensiek et al. (1979) for $HT^{-1} > 1.4$ both lend credence to the results. For $HT^{-1} > 1.4$, use of the Brakensiek et al. (1979) C_d values for nonsedimented conditions is recommended. For sedimented conditions, subtract 5.1% from the Brakensiek et al. (1979) C_d values as suggested by the scale-affected results reported herein because there is no alternative. When HT^{-1} is less than 1.4, values published herein for both the sedimented and nonsedimented cases should be used.

The assertion in Brakensiek et al. (1979) and repeated in the Water Measurement Manual (USBR 2001) that errors due to sediment accumulation are greatest for low heads is not consistent with the results reported herein. The authors found that the effect of sedimentation is significant and persists in most cases to $HT^{-1} > 3.4$, and can be as great as approximately 10% over a wide range of HT^{-1}.

Finally, use of the results presented in this study require that water level measurements be made at any location across the cross section, at a distance upstream from the weir face between $8 \leq xT^{-1} \leq 18$. Measurements nearer the channel bank are less likely to be affected by drawdown, which is at a maximum along the channel centerline. Because discharge coefficients in the present study are all adjusted to include the velocity head, users of these curves should develop some mechanism to estimate the velocity head in their channel at the water surface measurement point based on an estimated cross section and kinetic energy correction factor, unless the velocity head is negligible.

The tested sedimentation condition included a horizontal bed full of sediment to the invert of the weir with no live sediment transport. The effects of bed forms and live sediment transport remain for further study. The laboratory flow capacity limited testing to $HT^{-1} < 3.5$ for $\theta = 120°$ and $HT^{-1} < 3$ for $\theta = 140°$. Testing to higher values of HT^{-1} is needed. As the results show in Fig. 9, there is a need to perform tests at scales of at least 1:2 for the case of the USDA-ARS 140° weir for $HT^{-1} > 1.44$ to verify the intersection of the C_d values from the present study and the Brakensiek et al. (1979) curve. Given the lack of a single report describing the methodology and data used to develop the C_d values in Brakensiek et al. (1979), a study revisiting that topic near full scale using contemporary methods and error analysis techniques seems warranted. A scale of 1:1 or as near to it as possible should be used because scale effects were observed in the 3:16-scale model.

Acknowledgments

This study was largely funded using discretionary funds provided to the first author by the University of Wyoming as the Cline Distinguished Chair of Engineering, Environment, and Natural Resources at the University of Wyoming. Support for graduate, undergraduate, and high school student participation was provided by the U.S. National Science Foundation through Grants EAR-1045166, EPS-1135483, and EAR-1360384. This study was conceived and managed by the first author, who is responsible for the analysis presented in this paper. Coauthor Jesse Creel earned his M.S. thesis based on his study of the 120° Panama weir crest. Coauthor Ed Kempema served as laboratory manager during this study and kept the study and the students moving. Coauthor Trey Crouch and former M.S. student Juan Carlos Briceno showed the patience to reliably collect high-quality data day after day. Others who contributed to data collection in the lab from time to time include Michelle Ogden, former postdoctoral associate Nawa Raj Pradhan, former Ph.D. student Guy Litt, M.S. student Jason Regina, former M.S. student Nels Frazier, undergraduates Cornelus "Casey" Valkenburg, Samantha Marquard-Ogden, and Drew Herrera, and Emma Erikson and Fritz Ogden when they were high school students. This study would not have been possible without all their effort. Sherry Hunt and Ron Tejral of the USDA-ARS Hydraulic Engineering Research Unit provided key historical literature to aid in interpretation of past results. Reviewers Dave Goodrich and Tony Wahl contributed to the quality of this paper. Their attention to details is greatly appreciated.

Notation

The following symbols are used in this paper:

A = kinetic energy correction factor (Chow 1959);
C_d = discharge coefficient;
C_0, C_1 = constants in USDA rating equations from Manual 224 (Brakensiek et al. 1979);
g = acceleration due to gravity (LT^{-2});
H = total head above the weir invert (L);
h = height of water above the weir invert (L);
h_{max} = maximum flow height for weir (L);
m = divisor of T used in describing the weir crest shape; for the ARS weir crest $m = 8$, and for the Panama weir crest $m = 4$;
n = number of repeat experiments ($n \geq 4$);
P = vertical distance from weir invert to stream bed (L);
Q = discharge (L^3T^{-1});
S_o = bed slope;
s = sample standard deviation of ($n \geq 4$) C_d measurements;
T = thickness of short-crested weir (L) in the flow direction;
$t_{0.05,n-1}$ = t distribution at 0.05 significance level (95th percentile confidence interval) with $n - 1$ degrees of freedom;
V = average flow velocity (LT^{-1}); and
Θ = weir angle (radians).

References

Bos, M. G., ed. (1989). *Discharge measurement structures*, 3rd Ed., International Institute for Land Reclamation and Improvement, Wageningen, Netherlands.

Brakensiek, D. L., Osborn, H. B., and Rawls, W. J. (1979). "Field manual for research in agricultural hydrology." *Agriculture handbook 224*, USDA, Washington, DC.

Chow, V. T. (1959). *Open-channel hydraulics*, McGraw-Hill, New York.

Creel, J. N. (2013). "Effects of sedimentation on flow measurements from short crested triangular weirs." M.S. thesis, Dept. of Civil and Architectural Engineering, Univ. of Wyoming, Laramie, WY.

Ebben, W. P., Petushek, E. J., and Clewein, R. (2009). "A comparison of manual and electronic timing during 20 and 40 yard sprints." *J. Exer. Phys. Online*, 12(5), 34–39.

Gwinn, W. R., Ree, W. O., and DeCoursey, D. G. (1968). "The low-flow performance of broad-crested V-notch weirs." *Rep. SWC W5-eSt-2-14*, USDA, Agriculture Research Service, Stillwater, OK, 51–76.

Harrold, L. L., and Krimgold, D. B. (1943). "Devices for measuring rates and amounts of runoff." *SCS-TP-51*, USDA, Washington, DC.

Holtan, H. N., Minshall, N. E., and Harrold, L. L. (1962). "Field manual for research in agricultural hydrology." USDA, Washington, DC.

Hudson, J. A. (2004). "The impact of sediment on open channel flow measurement in selected UK experimental basins." *Flow Meas. Instrum.*, 15(1), 49–58.

Huff, A. N. (1938). "Tests of 16-inch weir and comparison with 30-inch weir." *Rep. No. 1*, Cornell Univ., Ithaca, NY.

Huff, A. N. (1941a). "Calibration of 2:1 V-notch measuring weirs." *Rep. No. MN-R-3-6*, St. Anthony Falls Hydraulic Laboratory, Minneapolis.

Huff, A. N. (1941b). "Calibration of 3:1 V-notch measuring weirs." *Rep. No. MN-R-3-8*, St. Anthony Falls Hydraulic Laboratory, Minneapolis.

Huff, A. N. (1942). "Calibration of 3:1 and 5:1 V-notch measuring weirs, supplement to calibration of 2:1 V-notch measuring weirs." *Rep. No. MN-R-3-7*, St. Anthony Falls Hydraulic Laboratory, Minneapolis.

LabVIEW [Computer software]. National Instruments Corporation, Austin, TX.

Mefford, B. W. (1979). "Rating broad crested V-notch weirs for different approach channels, 1979." M.S. thesis, Dept. of Civil Engineering, Colorado State Univ., Fort Collins, CO.

Montgomery, D., Runger, G., and Hubele, N. (2007). *Engineering statistics*, 4 Ed., Wiley, Hoboken, NJ.

Ogden, F. L., Crouch, T. D., Stallard, R. F., and Hall, J. S. (2013). "Effect of land cover and use on dry season river runoff and peak runoff in the seasonal tropics of central Panama." *Water Resour. Res.*, 49(12), 8443–8462.

Ree, W. O., and Gwinn, W. R. (1959). "The Virginia V-notch weir." *ARS-S-41-10*, Agricultural Research Service, USDA, Washington, DC.

Saxton, K. E., and Ruff, J. F. (1976). "Gaging sediment-laden flows with V-notch weirs." ⟨http://pubs.usgs.gov/misc/FISC_1947-2006/pdf/1st-7thFISCs-CD/3rdFISC/3Fisc-7.PDF#page=45⟩ (May 23, 2016).

Shapiro, S. S., and Wilk, M. B. (1965). "An analysis of variance test for normality (complete samples)." *Biometrika*, 52(3–4), 591–611.

USBR (U.S. Bureau of Reclamation). (2001). "Water measurement manual." ⟨http://www.usbr.gov/tsc/techreferences/mands/wmm/index.htm⟩ (Apr. 14, 2016).

WMO (World Meteorological Organization). (1971). "Use of weirs and flumes in stream gauging." *Technical Note No. 117*, Geneva.